**EPJ manuscript No.**
(will be inserted by the editor)

# How do small differences in nonidentical pulse-coupled oscillators induce great changes in their synchronous behavior?

G.M. Ramírez Ávila[1,a], J. Kurths[2,3,4], J.L. Guisset[5], and J.L. Deneubourg[5]

[1] Instituto de Investigaciones Físicas. Casilla 8635 Universidad Mayor de San Andrés, La Paz, Bolivia
[2] Institut für Physik. Humboldt-Universität zu Berlin, Robert-Koch-Platz 4, 10115, Berlin, Germany
[3] Potsdam Institut für Klimafolgenforschung. P.O. Box 60 12 03, 14412 Potsdam, Germany
[4] Institute for Complex Systems and Mathematical Biology. University of Aberdeen, Aberdeen AB24 3FX, United Kingdom
[5] Interdisciplinary Center for Nonlinear Phenomena and Complex Systems & Unité d'Ecologie Sociale. CP 231 Université Libre de Bruxelles, Campus de la Plaine, Bld. du Triomphe. Brussels, Belgium

**Abstract.** We studied synchronization and clustering in two types of pulse-coupled oscillators, namely, integrate-and-fire and light-controlled oscillators. We considered for the analysis globally coupled oscillators, either by a mean-field type coupling or a distance-dependent one. Using statistically diverse measures such as the transient, probability of total synchronization, fraction of clustered oscillators, mean size, and mean number of clusters, we describe clustering and synchronous behavior for populations of nonidentical oscillators and perform a comparative analysis of the behavioral differences and similitudes among these types of oscillators. Considering a mean-field approach, we found high probability of total synchronization in all cases for integrate-and-fire oscillators; on the other hand, in a more realistic situation, for light-controlled oscillators, i.e., when oscillators do not fire instantaneously, the probability of total synchronization decreases drastically for small differences among the oscillators and subsequently, for larger differences, it slightly increases. When the coupling strength depends on the distance, the probability of total synchronization plummets dramatically with the number of oscillators especially in the case of integrate-and-fire oscillators. The latter constitutes an interesting result because it indicates that in realistic situations, the probability of total synchronization is not very high for a population of pulse-coupled oscillators; this entails that its utilization as a paradigmatic model of total synchronization does not suit well, especially when the coupling depends on the distance. This article is dedicated to our good friend and colleague Hilda Cerdeira as a tribute to the scientific work developed over her career.

## 1 Introduction

The adjustment of rhythms of two or more oscillators due to a coupling between them is known as synchronization [1], a phenomenon which is widespread in systems of very diverse nature. Its study has deserved numerous publications dealing with theoretical and practical aspects. A review of synchronization theory can be found in [1–6] and its relation to complex networks in [7,8].

Synchronization of pulse-coupled oscillators has generated a lot of interest due to its applications related to biological systems such as the functionality of cardiac cells [9] and neurons [10], and the courtship of fireflies [11].

Integrate-and-fire oscillator (IFO) constitutes a paradigmatic model of pulse-coupled oscillators. Since its introduction by Mirollo and Strogatz [12], many theoretical contributions have been devoted to the study of synchronization of these oscillators, including aspects such as collective synchronization [13], inhibitory coupling [14], synchronization analysis of locally [15] and globally [16] coupled IFOs and its relation to self-organized criticality, synchronization time determination [17], slow switching in all-to-all delayed couplings [18], and synchronization when it is regulated or tuned by the movement of the oscillators [19–21], among others.

One of the most astonishing phenomena in nature is the synchronous flashing of certain firefly species [22], in particular in species of Thailand [23], New Guinea [24], North America [25,26], and Brazil [27]. This phenomenon has inspired several mathematical models [12,28], and also some electronic devices mimicking this behavior, like light-controlled oscillators (LCOs) [29]. These LCOs have been widely studied in several respects, e.g., synchronization in linear configurations [30], Arnold tongues determination [31], and noise effects [32,33]. Furthermore, LCOs have been recently applied to the complete courtship process, i.e., synchronization of males and the consequent response of females [11]. The underlying model for LCOs arises from the validation of experimental results [29,34] and in this sense we can affirm that these LCOs constitute realistic oscillators.

In a certain way, IFOs and LCOs are similar but they differ in a primordial aspect, the firing process which is instantaneous in an IFO, contrary to the LCO's case, in which the firing is related to the duration of the flash emitted by an LCO that constitutes the possible coupling with other LCOs.

In this work, we consider globally coupled LCOs and IFOs, both described in Sect. 2. We analyze in Sect. 3, the probability of total synchronization ($PTS$), underlying transients (synchronization time) and clustering in populations of identical and nonidentical oscillators ranging from 2 to 25 oscillators and considering two types of coupling, namely, a mean-field and a distance-dependent coupling. In Sect. 4, we describe the methods and we also discuss the most important results by comparing the different cases and strengthening the differences of synchronous and clustering behavior for the considered oscillators. Finally, in Sect. 5, we summarize the results giving conclusions and perspectives.

## 2 General description of the oscillators and the coupling schemes

The oscillators that we deal with in this paper are individually considered as relaxation oscillators due to their intrinsics characteristics of having two different time scales, i.e., within each cycle there is an integrating (slow) process followed by a firing (fast) process. Each process ends at its own threshold. The form of the oscillation is very different from a sinusoidal wave; rather it resembles a sequence of pulses. As it

[a] e-mail: gramirez@ulb.ac.be

was stated above, the general feature of relaxation oscillators is the slow growth of some quantity and its fast resetting at a threshold [1].

### 2.1 Light-controlled oscillators

These oscillators were introduced for the first time with the aim of mimicking fireflies behavior [35,36]; the model and its validation from experimental results are shown in [29]. The main feature of an LCO consists in its emission of pulses of light by one or several LEDs during its firing process and this fact allows a pulsatile coupling with other LCOs that can receive these pulses by means of some photodiodes. The oscillatory features of an LCO are given by simple electronics components in which a chip LM555 establishes two well-defined lower ($V_M/3$), and upper ($2V_M/3$) thresholds, where the discharging stage changes to the charging one and vice versa when one of these thresholds is achieved; $V_M$ being the voltage source. These stages are associated to a binary variable $\epsilon(t)$. The time intervals lasting for the charging (slow process with $\epsilon(t) = 1$) and the discharging (fast process with $\epsilon(t) = 0$) are characterized by the values of the resistors $R_\lambda$ and $R_\gamma$ respectively, and also by the capacitor $C$ of two $RC$ circuits related to these processes. Furthermore, considering that LCOs are mutually coupled with a coupling strength $\beta_{ij}$ that represents the pulsatile action of the $\mathrm{LCO}_j$'s flash over the $\mathrm{LCO}_i$ that occurs during the discharging of the $\mathrm{LCO}_j$. Concurrently, $\beta_{ij}$ are the elements of the weighted adjacency matrix of the set [37]. The dynamical equations describing a set of $N$ coupled LCOs are:

$$\frac{\mathrm{d}V_i(t)}{\mathrm{d}t} = \lambda_i[V_{Mi} - V_i(t)]\epsilon_i(t) - \gamma_i V_i(t)[1 - \epsilon_i(t)] + \sum_{j=1}^{N} \beta_{ij}[1 - \epsilon_j(t)] \ , \qquad (1)$$

where $\lambda_i$ and $\gamma_i$ are coefficients related to the electric components of the $RC$ circuits and are given by $\lambda_i = \frac{1}{(R_{\lambda i}+R_{\gamma i})C_i}$ and $\gamma_i = \frac{1}{R_{\gamma i}C_i}$. By integrating Eq. (1) and taking into account the thresholds introduced above, the natural period of an LCO, i.e., when it is not coupled to other LCOs, might be straightforwardly computed as $T_{0i} = T_{0\lambda i} + T_{0\gamma i} = (R_{\lambda i} + 2R_{\gamma i})C_i \ln 2$, where $T_{0\lambda i} = \frac{\ln 2}{\lambda_i}$ and $T_{0\gamma i} = \frac{\ln 2}{\gamma_i}$ are, respectively, the lasting time for the charge and the discharge when there is no action on the $\mathrm{LCO}_i$ by other LCOs. A simple inspection of Eq. (1) shows that both charging and discharging stages might be modified by the effect of the coupling with other LCO(s). The charging and the discharging times might be shortened or lengthened respectively when the pulsatile action due to the light of other LCOs takes place.

### 2.2 Integrate-and-fire oscillators

These oscillators are very well-known due to their simplicity and the easy way in which they achieve synchronization, as proved in [12] for identical globally coupled IFOs. The dynamics of an IFO is very simple and might be described in terms of some real valued state variable, increasing monotonically up to a threshold ($V_i = 1$). When the threshold is reached, the IFO relaxes to its baseline ($V_i = 0$) firing an instantaneous pulse that affects the dynamics of the IFOs coupled to it in an excitatory way, i.e., shortening the duration to reach their respective thresholds [38]. In its pristine form, a group of $N$ IFOs is described by

$$\frac{\mathrm{d}V_i(t)}{\mathrm{d}t} = I_i - \eta_i V_i(t), \quad 0 \leq V_i(t) \leq 1, \quad i = 1, \ldots, N \ . \qquad (2)$$

The oscillators are pulse-coupled and whether the $\mathrm{IFO}_j$ reaches its threshold, it fires and the variables $V_i$ of all the other IFOs are modified by adding the quantity $\beta_{ij}$ but not exceeding the threshold $V_i = 1$, i.e., $V_i(t^+) = \min(1, V_i(t) + \beta_{ij})$. A general coupling scheme in which it is possible that a set of $N_f < N$ IFOs achieve simultaneously their thresholds, implies that $\mathrm{IFO}_i$ modifies its dynamics in the form:

$$\textbf{If } \{V_j(t) = 1\} \Longrightarrow V_i(t^+) = \min\left(1, V_i(t) + \sum_{j=1}^{N_f} \beta_{ij}\right) \wedge \left\{V_j(t^+) = 0\right\} \ , \tag{3}$$

where $j = 1, \ldots, N_f$. Hereinafter, it is understood that the above mentioned condition is applied to all the equations related to IFOs, i.e., Eqs. (5), (7) and (9). The meaning of $\beta_{ij}$ is the same as that in the LCOs' case. The integration of Eq. (2) gives the natural period of an IFO: $T_{0i} = \frac{1}{\eta_i} \ln \frac{I_i}{I_i - \eta_i}$. As we wish to compare LCOs and IFOs, we can modify the IFOs' equations in order to put them in terms of the same variables and parameters used for the LCOs. Thus, the equations describing the dynamics of $N$ IFOs might be rewritten as:

$$\frac{\mathrm{d}V_i(t)}{\mathrm{d}t} = \lambda_i'[V_{Mi} - V_i(t)], \quad \frac{V_{Mi}}{3} \leq V_i(t) \leq \frac{2V_{Mi}}{3} \ , \tag{4}$$

with $\lambda_i' = \frac{1}{T_{0i}} = \frac{\lambda_i}{1 + R_{\gamma i} C_i \lambda_i}$.

When IFOs are coupled, we have similarly to Eq. (3)

$$\textbf{If } \left\{V_j(t) = \frac{2V_{Mj}}{3}\right\} \Longrightarrow V_i(t^+) = \min\left(\frac{2V_{Mi}}{3}, V_i(t) + \sum_{j=1}^{N_f} \beta_{ij}'\right) \wedge \left\{V_j(t^+) = \frac{V_{Mj}}{3}\right\} \ . \tag{5}$$

In order that coupling strength may have the same features in LCOs and IFOs, $\beta_{ij}'$ might be written in terms of that for the LCOs as $\beta_{ij}' = \beta_{ij} T_{0\gamma j} = \beta_{ij} R_{\gamma j} C_j \ln 2$. Consequently, we have the equations governing the IFOs with the same characteristics of the LCOs. Thus, a comparison between LCOs and IFOs is now feasible. The typical values used in this work for the parameters are $V_M = 9.0$ V, $R_\lambda = 100.0$ k$\Omega$, $R_\gamma = 1.6$ k$\Omega$, and $C = 0.47$ $\mu$F.

### 2.3 Mean-field coupling

Since the pioneering work of Winfree [39] and Kuramoto [40] concerning the mean-field approach to study coupled oscillators, this concept has significantly advanced and developed when applying to maps [41–43] and continuous systems exhibiting chaotic behavior [44–46]. Numerous studies used this approach to describe synchronization in different kinds of systems [47–49], in particular in pulse coupled oscillators [12]. We use this approach by considering that all the oscillators are globally coupled (all-to-all coupling) and the mean-field acts in such a way that we can consider a single value for the coupling strength among all the oscillators. This concept is represented in a simple fashion in Fig. 1(a), where the most important fact is the uniformity of the coupling strength between each pair of oscillators, i.e., the coupling strength is independent of the oscillators' position in space and has a unique value. Note that for all these cases, we consider bidirectional and symmetric coupling whose value is given by $\frac{\beta}{N}$. Thus, the equations describing globally coupled LCOs under a mean-field approach are:

$$\frac{\mathrm{d}V_i(t)}{\mathrm{d}t} = \lambda_i[V_{Mi} - V_i(t)]\epsilon_i(t) - \gamma_i V_i(t)[1 - \epsilon_i(t)] + \frac{\beta}{N}\sum_{j=1}^{N}[1 - \epsilon_j(t)] \ , \tag{6}$$

while, for IFOs, the equations are always given by Eq. (4) with the condition that:

$$\textbf{If}\left\{V_j(t)=\frac{2V_{Mj}}{3}\right\}\Longrightarrow V_i(t^+)=\min\left(\frac{2V_{Mi}}{3},V_i(t)+\beta'\frac{N_f}{N}\right)\wedge\left\{V_j(t^+)=\frac{V_{Mj}}{3}\right\}\ . \tag{7}$$

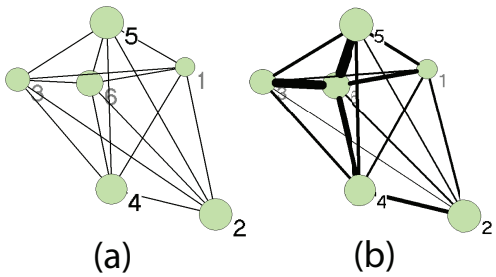


**Fig. 1.** Representation of all-to-all coupled oscillators (a) under a mean-field approach where the coupling strength is the same regardless the position of the oscillators or the distances between them. (b) Under an approach considering the coupling as distance-dependent.

### 2.4 Distance-dependent coupling

In order to study all-to-all distance-dependent coupling between oscillators (Fig. 1(b)), we firstly consider a "square" arena consisting of 2500 locations (50× 50 square cells); each of which can be occupied by an oscillator. Experimentally, the coupling strength ($\beta$) is found to be dependent on the distance ($r$) between the oscillators, as $\beta_{ij}\propto\frac{1}{r_{ij}^{\alpha}}$, where the exponent $\alpha$ was found to take the value 2.11 [29]. Hence, the equations governing a system of globally coupled LCOs are given by:

$$\frac{\mathrm{d}V_i(t)}{\mathrm{d}t}=\lambda_i(V_{Mi}-V_i(t))\epsilon_i(t)-\gamma_iV_i(t)[1-\epsilon_i(t)]+\ \beta_{\mathrm{ref}}\sum_{j=1}^{N}[1-\epsilon_j(t)]\left(\frac{r_{\mathrm{ref}}}{r_{ij}}\right)^{\alpha}\ , \tag{8}$$

where $\beta_{\mathrm{ref}}=166$, $r_{\mathrm{ref}}=4.85$ [cm] are respectively, the reference coupling strength and the reference distance taken from the model validation [29]. We also consider that minimal distance between LCOs is 1.8 cm, where this distance is determined by using the relationship: $r_{ij}\ =\ 1.8\ \sqrt{(x_i-x_j)^2+(y_i-y_j)^2}$ [cm].

The equations for IFOs are given by Eq. (4) with the condition:

$$\textbf{If}\left\{V_j(t)=\frac{2V_{Mj}}{3}\right\}\Longrightarrow V_i(t^+)=\min\left(\frac{2V_{Mi}}{3},V_i(t)+\beta'_{\mathrm{ref}}\sum_{j=1}^{N_f}\left(\frac{r_{\mathrm{ref}}}{r_{ij}}\right)^{\alpha}\right)$$
$$\wedge\ \left\{V_j(t^+)=\frac{V_{Mj}}{3}\right\}\quad,\quad\forall i\neq j\ . \tag{9}$$

## 3 Method and results

We focus our work on nonidentical oscillators and how the differences among them induce changes in their synchronous behaviour. We chose the following parameter

values to determine $\lambda_i$ and $\gamma_i$: $R_\gamma = 1.6$ k$\Omega$, $C = 0.47$ $\mu$F, $R_{\lambda i} = 100$ k$\Omega \pm \sigma$, where $\sigma$ is a random number taking from a normal distribution with $(\mu = 0, \sigma^2)$. Thus, we characterize the difference among the oscillators by means of the relative standard deviation $\sigma_{\text{rel}}$ related to $R_{\lambda i}$ defined as $\sigma_{\text{rel}} = \frac{\sigma}{100\ \text{k}\Omega}$.

According to the above mentioned parameter values, the oscillators' natural periods take the value $T_0 = 33.62$ ms $\pm\ \Delta T$, being $\Delta T$ the variation of the period related to $\sigma_{\text{rel}}$.

With the aim of studying the synchronous behavior of globally coupled LCOs and IFOs considering a mean-field coupling and a distance-dependent one, we performed, for each situation, 100 simulations with random initial conditions and random oscillators' positions, with between 2 and 25 oscillators characterized by the aforementioned parameter values and the variations featured by $\sigma_{\text{rel}}$ shown in Table 1. Concerning the integration time, we limit this to 15000 firing events. For all numeric experiments, we use a coupling strength $\beta = 166$. The number of numerical experiments that we carried out for each kind of oscillators was $100 \times 24 \times 11 \times 2 = 52800$, allowing statistical analyses. A particularly noteworthy feature is the small differences among the oscillators. The aspects to be analyzed are the following: probability of total synchronization, transients or synchronization time, and clustering.

**Table 1.** Chosen values of the variance related to $R_{\lambda i}$ and their consequent relative standard deviation $\sigma_{\text{rel}}$.

| $\sigma^2$ [$\Omega^2$] | 0 | 1 | 2 | 5 | 50 | 100 | 300 | 500 | 1000 | 3000 | 5000 |
|---|---|---|---|---|---|---|---|---|---|---|---|
| $\sigma_{\text{rel}}$ $\times 10^{-4}$ | 0 | 0.10 | 0.14 | 0.22 | 0.71 | 1.00 | 1.73 | 2.24 | 3.16 | 5.48 | 7.07 |

### 3.1 Probability of total synchronization

In order to study synchronization of coupled oscillators, we introduce the concept of probability of total synchronization ($PTS$), defined as the ratio of the number of trials in which all the oscillators achieve complete synchronization to the number of total trials. We use two criteria to study synchronization: the first refers to almost simultaneous firing events with constant phase differences, and the second evaluates the equality of periods as the criterion for synchronization. We respectively denote these criteria as the phase difference criterion (PDC) and the period criterion (PC). PDC is very strong, in the sense that it only considers as synchronized those oscillators flashing almost simultaneously and keeping their phase difference constant.

When considering a mean-field approach for LCOs and IFOs, we obtain numerical results of the $PTS$ using PDC and PC. Those results are shown in Fig. 2. We observe that there are very slight differences concerning the $PTS$ when the oscillators are identical; in the case of LCOs (Fig. 2(a)), the $PTS$ is mostly the same regardless the use of PC or PDC and always greater than 80%; and for the IFOs (Fig. 2(k)) $PTS_{\%} \approx 100\%$ for both criteria and independent of $N$. Furthermore, for IFOs, $PTS_{\%} \approx 100\%$ , without regard to the intrinsic differences among the IFOs characterized by $\sigma_{\text{rel}}$ as seen in Fig. 2(l). This behavior of complete synchronization in IFOs is in accordance with that obtained in [12,17,38]. For small LCOs' differences $\sigma_{\text{rel}} \leq 0.71 \times 10^{-4}$, the $PTS$ plummets dramatically for both criteria (Fig. 2(b)-(c)). On the other hand, for $\sigma_{\text{rel}} > 0.71 \times 10^{-4}$ (Fig. 2(d)-(j)) there is a tendency for the $PTS$ to increase, especially when considering PC. The differences exhibited on $PTS$ values when using PC and PDC are due to the fact that in the PC case, anti-synchronization and phase synchronization are also included.

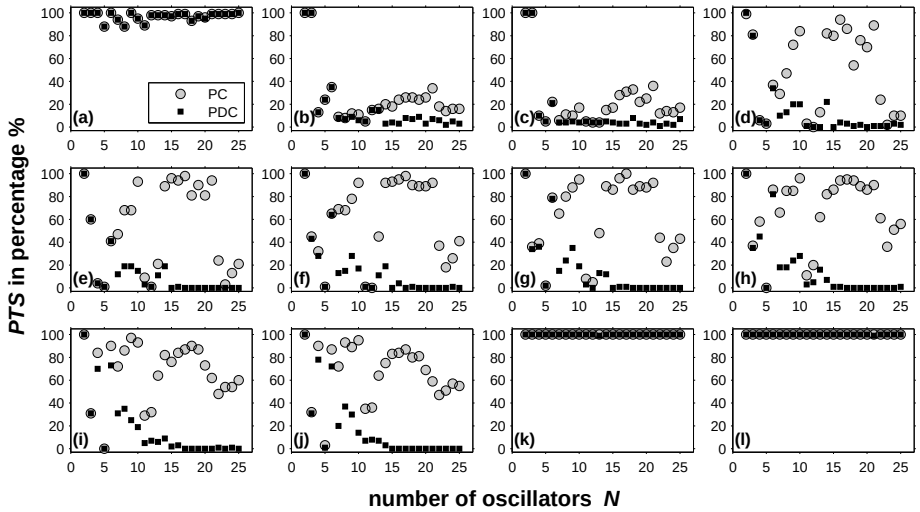


**Fig. 2.** Probability of total synchronization ($PTS$) in percentage as a function of $N$ for a mean-field approach, using the PC (gray circles) and PDC (black squares) for different $\sigma_{\rm rel}$ related to LCOs (a) 0 (identical), (b) $0.10\times10^{-4}$, (c) $0.22\times10^{-4}$, (d) $0.71\times10^{-4}$, (e) $1.00\times10^{-4}$, (f) $1.73\times10^{-4}$, (g) $2.24\times10^{-4}$, (h) $3.16\times10^{-4}$, (i) $5.48\times10^{-4}$, (j) $7.07\times10^{-4}$, and related to IFOs (k) 0 (identical), and (l) $7.07\times10^{-4}$.

When the coupling depends on the distance, there is a major change in the oscillators' behavior as shown in Fig. 3, where the $PTS$ falls sharply with $N$ even for identical LCOs (Fig. 3(a)) and IFOs (Fig. 3(k)). For both types of oscillators, the intrinsic differences $\sigma_{\rm rel}$ exacerbate the $PTS$ fall as seen in the sequence Fig. 3(b)-(j) for LCOs and in Fig. 3(l) for IFOs. According to the shape in which $PTS$ plummets, we can adjust the data of each kind of oscillators and for each criterion to an exponential function $PTS(N) = PTS(2)\mathrm{e}^{-k(N-2)}$, where $PTS(N)$ is the probability of total synchronization when the set is composed of $N$ oscillators. It is clear that $PTS(2)$ declines with $\sigma_{\rm rel}$.

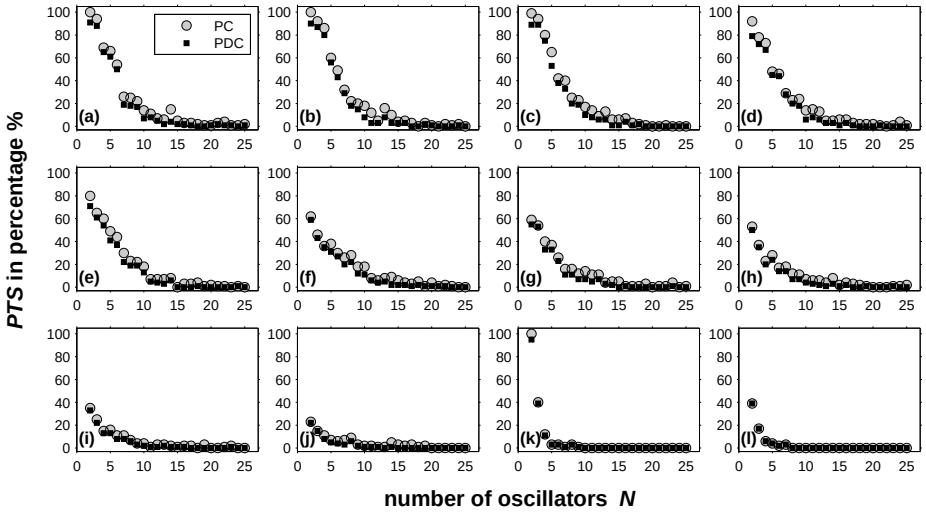


**Fig. 3.** Idem as Fig. 2 but for a distance-dependent coupling.

### 3.2 Transients

An interesting issue when studying synchronization is that related to the transient, i.e., the time in which all the elements of the system synchronize. Transients or synchronization times were studied numerically in locally coupled LCOs [50] and IFOs [17], and in identical globally coupled LCOs and IFOs [51]. In order to study transients, we consider PDC as the criterion to determine whether or not a set of oscillators achieves total synchronization. When the coupling is a mean-field one, we observe in the scatter plots of Fig. 4 that for identical LCOs (Fig. 4(a)) and IFOs (Fig. 4(e)), mostly the whole populations synchronize, in accordance with the statement in Sect. 3.1. Note that circles' sizes are proportional to the $PTS$ in percentage. The transient grows with $N$ but the mean values are small for both cases. On the contrary, when we consider the differences $\sigma_{\text{rel}}$, we observe for LCOs that transient swells significatively with $N$ but also, $PTS$ slumps with $N$. When the coupling depends on

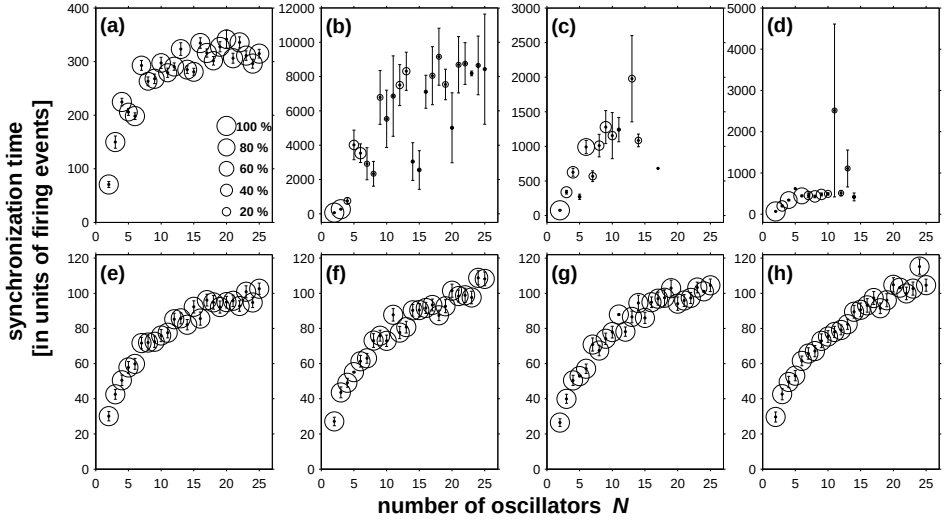


**Fig. 4.** Synchronization time as a function of $N$ for globally coupled LCOs (top) and IFOs (bottom) being the coupling a mean-field one, when the differences $\sigma_{\text{rel}}$ are: (a) and (e) 0 (identical), (b) and ((f) $0.10\times10^{-4}$, (c) and (g) $2.24\times10^{-4}$, and (d) and (h) $7.07\times10^{-4}$. The size of the circles are proportional to $PTS$ and the error bars represent the standard deviation.

the distance between oscillators, synchronization time escalates even when the oscillators are identical (Fig. 5(a) and (f)). The case of identical IFOs is dramatic inasmuch as populations with $N > 8$ implies noughts for the $PTS$. The same behavior in both kind of oscillators is observed when the diferences are $\sigma_{\text{rel}} = 0.10 \times 10^{-4}$ (Fig. 5(b) and (f)), $\sigma_{\text{rel}} = 2.24 \times 10^{-4}$ (Fig. 5(c) and (g)), and $\sigma_{\text{rel}} = 7.07 \times 10^{-4}$ (Fig. 5(d) and (h)). It is remarkable that complete synchronization is not usual when the coupling is distance-dependent.

### 3.3 Clustering

A great number of works dealing with clustering can be found in the literature and in diverse fields, going from biological phenomena related to insects behavior [52] to

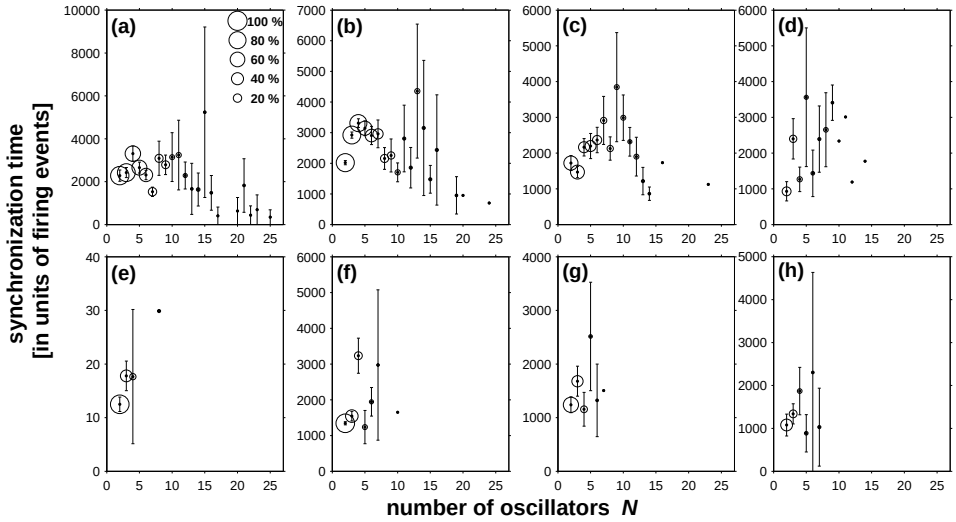


**Fig. 5.** Idem as Fig. 4 but for a distance-dependent coupling.

physical ones [53], including several applications to networks [54–56] and synchronization [57–59]. Clustering might be defined as the coherent groups formation as a result of the interaction between the elements of a population, being this phenomenon a form of self-organization [3].

We analyze the clustering behavior on populations of LCOs and IFOs when the set of oscillators does not necessarily achieve total synchronization (all the oscillators synchronized). In order to study clustering, we use PC as the criterion to determine the clusters' features, i.e., we consider a cluster as an ensemble of synchronized oscillators sharing the same period. We choose four features to describe the clustering, namely:

Mean fraction of aggregated individuals: represents the mean value of the ratio of the oscillators who are part of a cluster compared to the total population evaluated for all performed experiments.

Normalized mean size of the biggest cluster: is the mean value of the ratio between the biggest cluster found in each experiment and the whole population of oscillators.

Mean number of clusters: describes the mean value of the number of clusters found in each experiment.

Mean size of clusters: represents the averaged value of the clusters' size found in each experiment.

As in the precedent analysis, we consider populations of oscillators ranging from 2 to 25 for which we perform 100 simulations with random initial conditions. We compute the clustering features, some of those are shown in Fig. 6. Considering mean-field coupled LCOs, we observe strong changes concerning the fraction of clustered oscillators (first row of Fig. 6) and the normalized size of the biggest cluster (third row of the Fig. 6) even for very small differences $\sigma_{\text{rel}} = 0.10 \times 10^{-4}$ as shown in Fig. 6(b) where the fraction of clustered LCOs drops for $N$ in-between 3 and 8 and then, it climbs with $N$; in the case of the normalized biggest cluster (Fig. 6(j)), it drops until $N = 7$ and then, it levels out at around 0.5. For $\sigma_{\text{rel}} = 2.24 \times 10^{-4}$ and $\sigma_{\text{rel}} = 7.07 \times 10^{-4}$ (Fig. 6(c)-(d) and (k)-(l)), there is a sharp fall until $N = 5$ and then these quantities grow intermittently with $N$, reaching in some cases values near to 1.0.

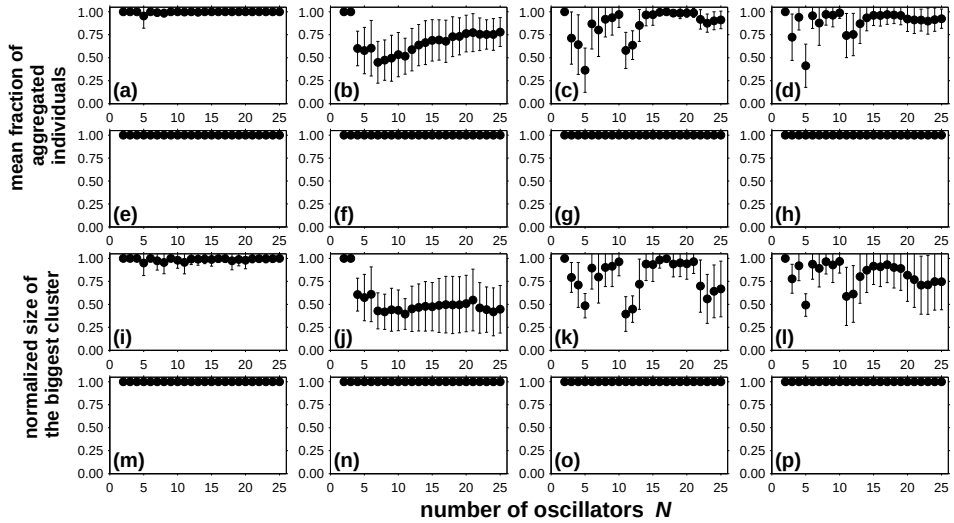


**Fig. 6.** Some clustering features as a function of the population size when the LCOs (first and third rows) and IFOs (second and fourth rows) are globally coupled considering a mean-field approach and differences given by $\sigma_{\text{rel}} = 0$ (identical), first column, i.e., (a), (e), (i) and (m); $\sigma_{\text{rel}} = 0.10 \times 10^{-4}$, second column, (b), (f), (j) and (n); $\sigma_{\text{rel}} = 2.24 \times 10^{-4}$, third column, (c), (g), (k) and (o); $\sigma_{\text{rel}} = 7.07 \times 10^{-4}$, fourth column, (d), (h), (l) and (p). Error bars are related to the standard deviation.

In the case of mean-field coupled IFOs, there are no changes neither in the fraction of clustered IFOs, nor in the size of the biggest cluster, regardless the value of $\sigma_{\text{rel}}$. In other words, a system of globally coupled IFOs under a mean-field coupling always achieves total synchronization.

When the coupling is distance-dependent, the clustering behavior is quite different compared to that related to mean-field coupling as shown in Fig. 7. For identical LCOs and $\sigma_{\text{rel}} = 0.10 \times 10^{-4}$, both the mean fraction of aggregated individuals (Fig. 7(b)) and the normalized size of the biggest cluster (Fig. 7(j)) fall steadily with $N$. When $\sigma_{\text{rel}} = 2.24 \times 10^{-4}$, the fraction of clustered LCOs drops markedly for $N = 2$, then it climbs until $N = 4$ and eventually, it falls off almost regularly (Fig. 7(c)). Finally, when $\sigma_{\text{rel}} = 7.07 \times 10^{-4}$, the fraction of clustered LCOs plummets dramatically for $N = 2$, then it increases until $N = 9$ and for $N \geq 10$, it slightly slackens (Fig. 7(d)). Concerning the normalized size of the biggest cluster, it varies inversely as $N$ (Fig. 7(i)-(l)).

Clustering of distance-dependent coupled IFOs shows that for identical IFOs and small differences, the fraction of clustered IFOs decreases for small $N$ and then it levels out at around 0.63 for larger $N$ (Fig. 7(e)-(g)); for $\sigma_{\text{rel}} = 7.07 \times 10^{-4}$, a similar behavior but with a sharp fall for small $N$ is observed (Fig. 7(h)) followed by a stabilization at around 0.63. Finally, concerning the normalized size of the biggest cluster for IFOs, in all cases, it declines with $N$ (Fig. 7(m)-(p)).

## 4 Discussion

From the results shown in Sect 3, we can perform a statistical comparison among the oscillators and the both types of coupling taking into account all the used values for $\sigma_{\text{rel}}$. In other words, with the aim of comparing, we express the mean values concerning all the studied quantities in Sect 3 as a function of $\sigma_{\text{rel}}$.

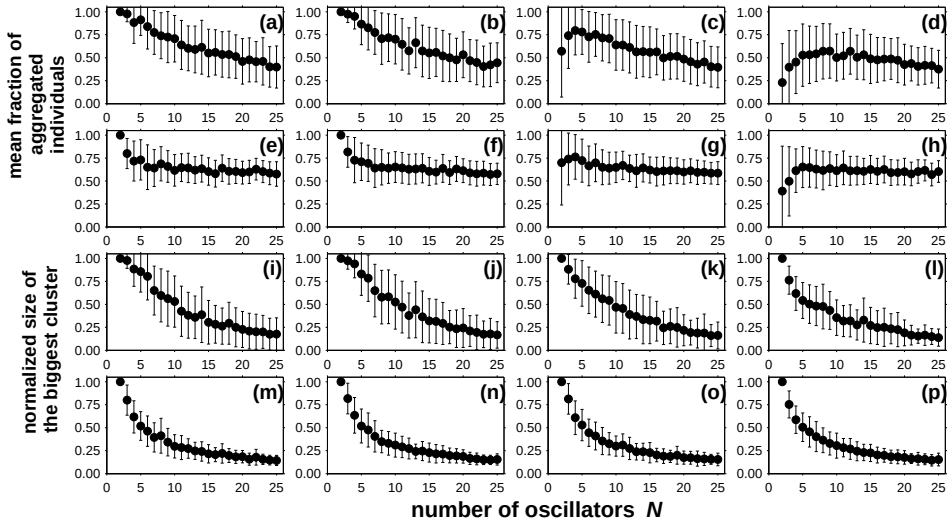


**Fig. 7.** Idem as Fig. 6 but for a distance-dependent coupling.

In order to compare the $PTS$, we compute the mean value of this quantity ($\langle PTS \rangle$) for all the configurations and then we express this as a function of $\sigma_{\text{rel}}$ as shown in Fig. 8. Concerning LCOs and mean-field coupling, from a statistical point of view, $\langle PTS \rangle$ declines dramatically for very small differences whether using PDC or PC, then $\langle PTS \rangle$ levels off when using PDC and increases until it reaches around 70% when using PC. When the coupling for the LCOs is distance-dependent, $\langle PTS \rangle$ is around 20% for identical LCOs and then it falls down slightly with $\sigma_{\text{rel}}$ as shown in Fig. 8(b); note that in this case, there is not a significative difference between the two criteria (PDC and PC). The $\langle PTS \rangle$ is mostly 100% for mean-field coupled IFOs and it is not affected by $\sigma_{\text{rel}}$ as Fig. 8(c) shows. When the coupling among IFOs is distance-dependent, $\langle PTS \rangle$ is small even for $\sigma_{\text{rel}} = 0$; we observe from Fig. 8(d) that $\langle PTS \rangle$ falters slightly with $\sigma_{\text{rel}}$.

The comparison of transients is summarized in Fig. 9 (left black vertical axis for LCOs, and right gray vertical axis for IFOs), where for mean-field coupling, the LCOs and the IFOs behaviors differ in several respects: the mean value of the transient is quite larger for LCOs (it may exceed 6000 firing events) than for IFOs, where the synchronization time never exceeds 120 firing events. Additionally, we also see from Fig. 9(a) that circles' sizes (proportional to $\langle PTS \rangle$) are quite smaller for LCOs. A last observation is the statistical trend to diminish the transient with increasing $\sigma_{\text{rel}}$ but with $\langle PTS \rangle < 40\%$. For a distance-dependent coupling, there is no specific trend neither for LCOs, nor for IFOs as it is shown in Fig. 9(b).

In order to compare the changes in the clustering features among oscillators, we computed mean values of the four considered quantities taking into account all the configurations for the computation of these mean values. We represent these quantities as a function of $\sigma_{\text{rel}}$ as shown in Fig. 10.

Concerning the mean fraction of aggregated oscillators, when the coupling is a mean-field one, we observe from Fig. 10(a) that for LCOs, this quantity climbs with $\sigma_{\text{rel}}$ and then it levels out at around 0.9. For IFOs, the mean fraction of aggregated individuals is always 1.0 regardless of the $\sigma_{\text{rel}}$ values. On the contrary, when the coupling depends on the distance, the mean fraction of clustered oscillators decreases with $\sigma_{\text{rel}}$ uniformly for LCOs and slightly for IFOs (Fig. 10(b)).

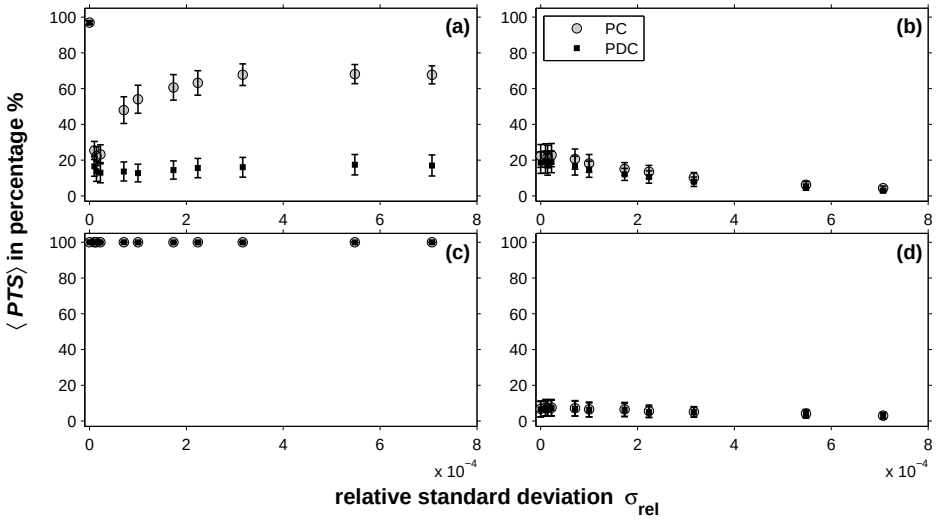


**Fig. 8.** Comparison using $\langle PTS \rangle$ in percentage as a function of the differences among oscillators $\sigma_{\mathrm{rel}}$ considering four situations of globally coupled oscillators: (top: LCOs) (a) mean-field and (b) distance-dependent coupling. (bottom: IFOs) (c) mean-field and (d) distance-dependent coupling. The gray circles indicate the use of PC and the black squares, that of PDC. Error bars represent the mean squared errors.

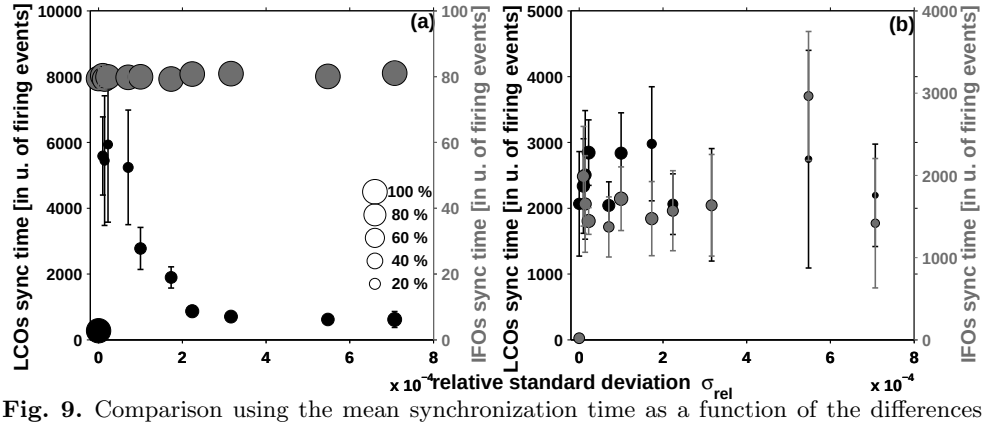


**Fig. 9.** Comparison using the mean synchronization time as a function of the differences among the oscillators $\sigma_{\mathrm{rel}}$. (a) Mean field coupling, and (b) distance-dependent coupling. The left vertical axis and the black circles describe the LCOs, whereas the right vertical axis and the gray circles describe the IFOs. The size of the circles is related to $PTS$. Error bars represent the standard deviation.

Regarding to the normalized mean size of the biggest cluster, we see that this quantity behaves similarly as the mean fraction of clustered oscillators under a mean-field coupling, i.e., for LCOs it rises with $\sigma_{\mathrm{rel}}$ until it reaches a value around 0.8. For the IFOs, this quantity is always equal to 1, that is still a manifestation of total synchronization (Fig. 10(c)). When the coupling is distance-dependent, the normalized mean size of the biggest cluster for IFOs is practically constant and close to 0.35 and for LCOs it decreases regularly with $\sigma_{\mathrm{rel}}$ and approaches the value 0.35 (Fig. 10(d)).

With respect to the mean size of clusters, for mean-field coupled IFOs, the value of this quantity is constant and approximately equal to 13.5 that is the result to perform $\sum_{i=2}^{25} i/24$, whereas for LCOs it increases until around 9 and then it slightly declines

with the trend to level out near to 8 (Fig. 10(e)). When the coupling depends on the distance, the mean size of clusters for IFOs remains constant near to 2.4, whereas for LCOs, it falls uniformly with $\sigma_{\text{rel}}$ towards 2.4 (Fig. 10(f)).

In regard to the mean number of clusters when the coupling corresponds to a mean-field one, for IFOs, this quantity does not change with $\sigma_{\text{rel}}$ and takes the value 1 as expected (Fig. 10(g)). For LCOs, the mean number of clusters drops with $\sigma_{\text{rel}}$ and then it levels off. When the coupling is distance-dependent, for both LCOs and IFOs, the mean number of clusters remains practically constant as shown in Fig. 10(h). We

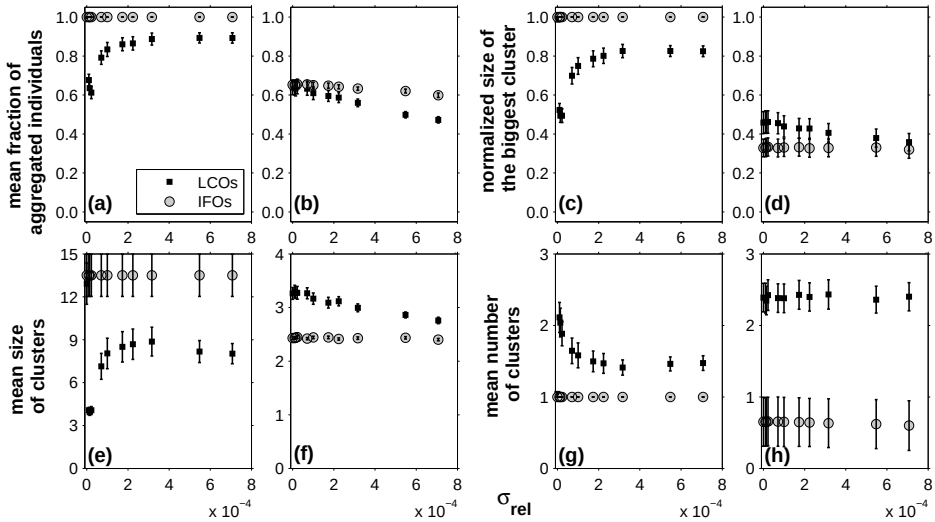


**Fig. 10.** Comparison using the clustering features as a function of the differences among the oscillators $\sigma_{\text{rel}}$. Mean fraction of aggregated oscillators for (a) mean-field, and (b) distance-dependent coupling. Normalized size of the biggest cluster for (c) mean-field, and (d) distance-dependent coupling. Mean size of clusters for (e) mean-field, and (f) distance-dependent coupling. Mean number of clusters for (g) mean-field, and (h) distance-dependent coupling. In all cases, the LCOs' features are characterized by black squares and those to IFOs by gray circles. Error bars are related to mean squared errors.

finish the comparison by constructing a table that summarizes the substantial changes in $\langle PTS \rangle$, synchronization time, and clustering features when two configurations are compared (see Table 2).

**Table 2.** Comparison of different coupling configurations of LCOs and IFOs and the possible great changes concerning the $\langle PTS \rangle$, the synchronization time and the clustering features. The check mark points out the existence of an important change in the concerned variable.

| configurations comparison | $\langle PTS \rangle$ | sync. time | clustering |
|---|---|---|---|
| LCOs mean-field vs. LCOs distance-dependent | ✓ | ✓ | ✓ |
| LCOs mean-field vs. IFOs mean-field | ✓ | ✓ | ✓ |
| LCOs mean-field vs. IFOs distance-dependent | ✓ | ✓ | ✓ |
| LCOs distance-dependent vs. IFOs mean-field | ✓ | ✓ | ✓ |
| LCOs distance-dependent vs. IFOs distance-dependent | | ✓ | |
| IFOs mean-field vs. IFOs distance-dependent | ✓ | ✓ | ✓ |

## 5 Conclusions and perspectives

The numerical toil performed in this work allows us to compare the synchronous and clustering behavior on four different configurations of pulse-coupled oscillators. In almost all cases, we found important differences despite those are similar in several respects. We remark that for mean-field coupled IFOs, the sets of these coupled oscillators always achieve total synchronization and in this sense, it is natural that they have been used to model different kinds of synchronous systems. Nevertheless, IFOs are not realistic oscillators. On the contrary, LCOs are realistic oscillators and despite they are quite similar to IFOs, their behavior is completely different, especially when the set of oscillators is composed of slightly different LCOs. Another important aspect that deserves to be pointed out is the type of coupling. In real systems, the coupling generally depends on the distance and consequently we should expect a cluster formation of synchronized individuals, rather than synchronization of the whole population. In summary, the use of real conditions (nonidentical oscillators without instantaneous firing and coupled by means of a distance-dependent coupling) not only allows us to obtain a better description of oscillatory systems but also shows an increase in the diversity of collective dynamics. It is interesting to note that LCOs and IFOs have a closer behavior when the coupling depends on the distance. The possible existence of a transition from LCOs to IFOs when LCOs' discharging time decreases going towards zero deserves currently our attention because the elucidation of this issue could helps us in the understanding of underlying aspects related to the synchronous behavior of these oscillators. This work could also be complemented by studying the influence of the coupling strength, noise and other dynamical aspects such as the possibility of oscillators motion.

J.K. acknowledges the German ministry for education and research (BMBF) via the project PROGRES. J.-L.D. is senior research associate from the Belgian National Fund for Scientific Research (FNRS).

## References

1. A. Pikovsky, M. Rosenblum, J. Kurths, *Synchronization : a universal concept in nonlinear sciences* (Cambridge University Press, New York, 2001)
2. S. Boccaletti, J. Kurths, G. Osipov, D.L. Valladares, C.S. Zhou, Phys. Rep. **366**(1-2), 1 (2002)
3. S.C. Manrubia, A.S. Mikhailov, D.H. Zanette, *Emergence of dynamical order* (World Scientific Publishing Co. Pte. Ltd., Singapore, 2004)
4. A. Balanov, N. Janson, D. Postnov, O. Sosnovtseva, *Synchronization: From Simple to Complex* (Springer Berlin, Berlin, 2007)
5. S. Boccaletti, *The Synchronized Dynamics of Complex Systems* (Elsevier, 2008)
6. A. Stefanski, *Determining thresholds of complete synchronization, and application* (World Scientific, 2009)
7. C.W. Wu, *Synchronization in Complex Networks of Nonlinear Dynamical Systems* (World Scientific Publishing Co. Pte. Ltd, London, 2007)
8. A. Arenas, A. Díaz-Guilera, J. Kurths, Y. Moreno, C. Zhou, Phys. Rep. **469**(3), 93 (2008)
9. C. Peskin, *Mathematical aspects of heart physiology* (1975)
10. N. Masuda, K. Aihara, Phys. Rev. E **64**(1), 051906 (2001)
11. G.M. Ramírez Ávila, J.L. Deneubourg, J.L. Guisset, N. Wessel, J. Kurths, Europhys. Lett. **94**(6), 60007 (2011)
12. R.E. Mirollo, S.H. Strogatz, SIAM J. Appl. Math. **50**(6), 1645 (1990)
13. Y. Kuramoto, Physica D **50**(1), 15 (1991)

14. C. Van Vreeswijk, L.F. Abbott, G.B. Ermentrout, J. Comput. Neurosci. **1**(4), 313 (1994)
15. A. Corral, C.J. Pérez, A. Díaz-Guilera, A. Arenas, Phys. Rev. Lett. **75**(20), 3697 (1995)
16. S. Bottani, Phys. Rev. Lett. **74**(21), 4189 (1995)
17. S.R. Campbell, D.L. Wang, C. Jayaprakash, Neural Comput. **11**(7), 1595 (1999)
18. H. Kori, Phys. Rev. E **68**(2), 021919 (2003)
19. S. Sarkar, Chaos **20**(4), 043108 (2010)
20. L. Prignano, O. Sagarra, P.M. Gleiser, A. Díaz-Guilera, Int. J. Bifurcat. Chaos **22**(07), 1250179 (2012)
21. L. Prignano, O. Sagarra, A. Díaz-Guilera, Phys. Rev. Lett. **110**(11), 114101 (2013)
22. J.B. Buck, Science **81**(2101), 339 (1935)
23. J. Buck, E. Buck, Science **159**(3821), 1319 (1968)
24. F.E. Hanson, J.F. Case, E. Buck, J. Buck, Science **174**, 161 (1971)
25. J. Copeland, A. Moiseff, J. Insect Behav. **8**(3), 381 (1995)
26. A. Moiseff, J. Copeland, J. Insect Behav. **13**(4), 597 (2000)
27. V.R. Viviani, Ann. Entomol. Soc. Am. **94**(1), 129 (2001)
28. B. Ermentrout, J. Math. Biol. **29**(6), 571 (1991)
29. G.M. Ramírez Ávila, J.L. Guisset, J.L. Deneubourg, Physica D **182**(3-4), 254 (2003)
30. G.M. Ramírez Ávila, J.L. Guisset, J.L. Deneubourg, J. Phys. CS **23**, 252 (2005)
31. N. Rubido, C. Cabeza, S. Kahan, G.M. Ramírez Ávila, A.C. Marti, Eur. Phys. J. D **62**(1), 51 (2011)
32. G.M. Ramírez Ávila, J.L. Guisset, J.L. Deneubourg, Int. J. Bifurcat. Chaos **17**(12), 4453 (2007)
33. G.M. Ramírez Ávila, J. Kurths, J.L. Guisset, J.L. Deneubourg, Phys. Rev. E **82**(5), 056207 (2010)
34. N. Rubido, C. Cabeza, A.C. Marti, G.M. Ramírez Ávila, Phil. Trans. R. Soc. A **367**, 32673280 (2009)
35. J.L. Guisset, G.M. Ramirez Avila, J.L. Deneubourg, Rev. Bol. Fis. **7**, 102 (2001)
36. J.L. Guisset, J.L. Deneubourg, G.M. Ramírez Ávila, arXiv.nlin.AO/0206036 (2002)
37. S. Boccaletti, V. Latora, Y. Moreno, M. Chavez, D.U. Hwang, Phys. Rep. **424**(4-5), 175 (2006)
38. S. Bottani, Phys. Rev. E **54**(3), 2334 (1996)
39. A.T. Winfree, J. Theor. Biol. **16**, 15 (1967)
40. Y. Kuramoto, I. Nishikawa, J. Stat. Phys. **49**(3-4), 569 (1987)
41. K. Kaneko, Prog. Theor. Phys. **74**(5), 1033 (1985)
42. G. Perez, S. Sinha, H.A. Cerdeira, Physica D **63**(3-4), 341 (1993)
43. A.S. Pikovsky, J. Kurths, Physica D **76**(4), 411 (1994)
44. M. Banaji, P. Glendinning, Phys. Lett. A **251**(5), 297 (1999)
45. I.Z. Kiss, Y. Zhai, J.L. Hudson, Phys. Rev. Lett. **88**(23), 238301 (2002)
46. S. de Monte, F. d'Ovidio, E. Mosekilde, Phys. Rev. Lett. **90**(5), 4102 (2003)
47. A.S. Pikovsky, M.G. Rosenblum, J. Kurths, Europhys. Lett. **34**(3), 165 (1996)
48. J.P. Gleeson, Europhys. Lett. **73**(3), 328 (2006)
49. N.F. Rulkov, L. Tsimring, M.L. Larsen, M. Gabbay, Phys. Rev. E **74**(5), 056205 (2006)
50. G.M. Ramírez Ávila, J.L. Guisset, J.L. Deneubourg, Rev. Bol. Fis. **12**, 1 (2006)
51. G.M. Ramírez Ávila, J.L. Guisset, J.L. Deneubourg, Rev. Bol. Fis. **13**, 1 (2007)
52. S. Depickère, G.M. Ramírez Ávila, D. Fresneau, J.L. Deneubourg, Ecol. Entomol. **33**(2), 225 (2008)
53. M. Nixon, M. Fridman, E. Ronen, A.A. Friesem, N. Davidson, I. Kanter, Phys. Rev. Lett. **108**(21), 214101 (2012)
54. A. Mauroy, R. Sepulchre, Chaos **18**(3), 037122 (2008)
55. D. Foster, J. Foster, M. Paczuski, P. Grassberger, Phys. Rev. E **81**(4), 046115 (2010)
56. J. Wu, L. Jiao, R. Li, W. Chen, Physica D **240**(24), 1972 (2011)
57. M. Escalona-Moran, M.G. Cosenza, P. Guillen, P. Coutin, Chaos Soliton Fract. **31**(4), 820 (2007)
58. P. Muruganandam, F.F. Ferreira, H.F. El-Nashar, H.A. Cerdeira, Pramana-J. Phys. **70**(6), 1143 (2008)
59. H.F. El-Nashar, H.A. Cerdeira, Commun. Nonlinear Sci. **16**(11), 4508 (2011)